Formation of liver metastases enhances the pro-cachectic signaling in colorectal cancer hosts

University of Colorado Anschutz Medical Campus

Chandler S. Callaway[1], Joshua R. Huot[2], Fabrizio Pin[2], Andrea Bonetto[1, 3]

[1] Department of Pathology, University of Colorado Anschutz Medical Campus, Aurora, CO, USA

[2] Department of Anatomy, Cell Biology & Physiology, Indiana University School of Medicine, Indianapolis, IN, USA

[3] University of Colorado Comprehensive Cancer Center, Aurora, CO, USA

Background

- Colorectal cancer (CRC) is a deadly disease that in its most advanced stages metastasizes to the liver and is accompanied by cachexia
- Cachexia is characterized by muscle and fat wasting, systemic inflammation, and reduced survival[1]
- Formation of liver metastases (LMs) accelerates cancer cachexia in tumor-bearing hosts[2]

1. Baracos VE, Martin L, Korc M, Guttridge DC, Fearon KCH. Cancer-associated cachexia. Nat Rev Dis Primers. 2018;4:17105.

2. Huot JR, Novinger LJ, Pin F, Bonetto A. HCT116 colorectal liver metastases exacerbate muscle wasting in a mouse model for the study of colorectal cancer cachexia. Dis Model Mech. 2020;13.

Methods

- 8-week-old male NSG mice were injected subcutaneously with human HCT116 CRC cells, or intrasplenically (mHCT116) to model the dissemination of LMs
- Livers and tumors from the subcutaneous and metastatic models, alongside their respective controls, were collected and RNA sequencing performed
- Animals were assessed for muscle force 24-hours prior to euthanasia, and skeletal muscles were collected for mass and morphological analyses.
- Co-culture of hepatocytes (AML12) and CRC cells (HCT116) was then modelled in vitro and conditioned media used to treat C2C12 myotubes.

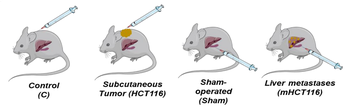

Figure 1: LMs worsen CRC-induced body wasting

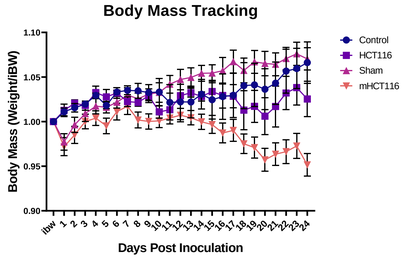

Figure 1: HCT116 cells were implanted subcutaneously (HCT116, 3.0×10^6) or intrasplenically (mHCT116, 1.25×10^5) and body mass was recorded daily and normalized to initial body mass (iBW). Control n=4, HCT116 n=5, Sham n=6, mHCT116 n=10

Figure 2: LMs aggravate CRC-induced cachexia phenotype

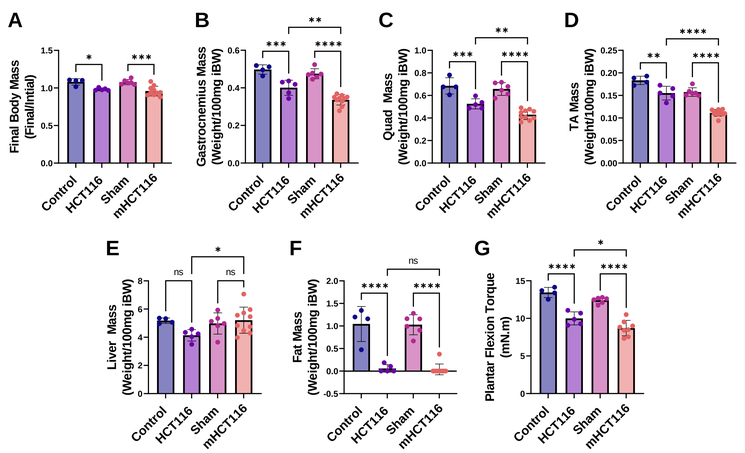

Figure 2: **(A)** Final body, **(B)** gastrocnemius muscle, **(C)** quadricep muscle, **(D)** tibialis anterior muscle, **(E)** liver, and **(F)** fat mass normalized to initial body weight (iBW). **(G)** In Vivo plantarflexion force assessment expressed as absolute force. Data are expressed as mean ± SD. Significance of the differences: *p<0.05, **p<0.01, ***p<0.001, ****p<0.0001.

Figure 3: Metastasis formation alters the molecular landscape of liver during cancer

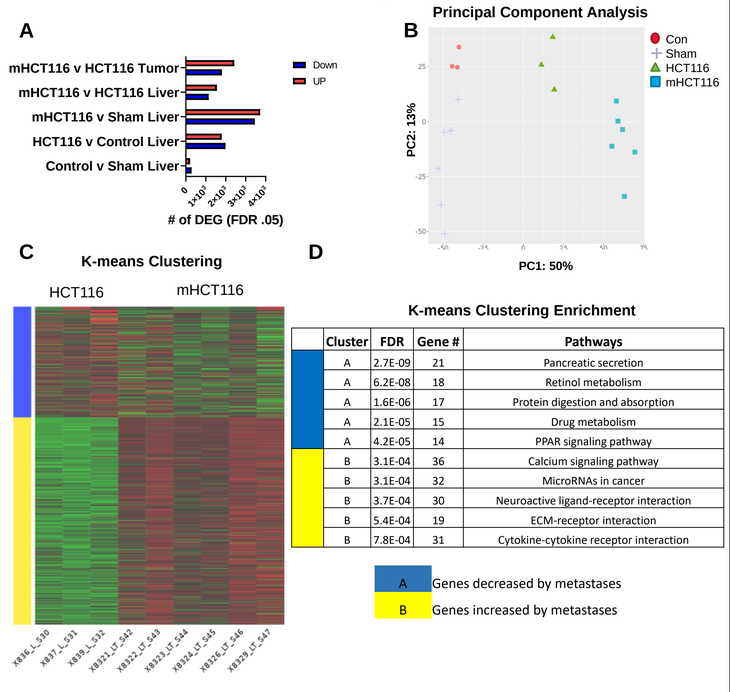

	Cluster	FDR	Gene #	Pathways
	A	2.7E-09	21	Pancreatic secretion
	A	6.2E-08	18	Retinol metabolism
	A	1.6E-06	17	Protein digestion and absorption
	A	2.1E-05	15	Drug metabolism
	A	4.2E-05	14	PPAR signaling pathway
	B	3.1E-04	36	Calcium signaling pathway
	B	3.1E-04	32	MicroRNAs in cancer
	B	3.7E-04	30	Neuroactive ligand-receptor interaction
	B	5.4E-04	19	ECM-receptor interaction
	B	7.8E-04	31	Cytokine-cytokine receptor interaction

Figure 3: **(A)** Number of Differentially Expressed Genes (DEGs) identified using an FDR-q <.05 for each comparison. **(B)** Principal component analysis plot for all Liver comparisons. **(C)** K-means clustering expressed as a heatmap of mHCT116 vs. HCT116 livers. (D) Top 5 significantly enriched KEGG pathways for genes in cluster A and B. Control n=3, HCT116 n=3, Sham n=6, mHCT116 n=6

Figure 4: Cachexia signaling is exacerbated in mHCT116 livers

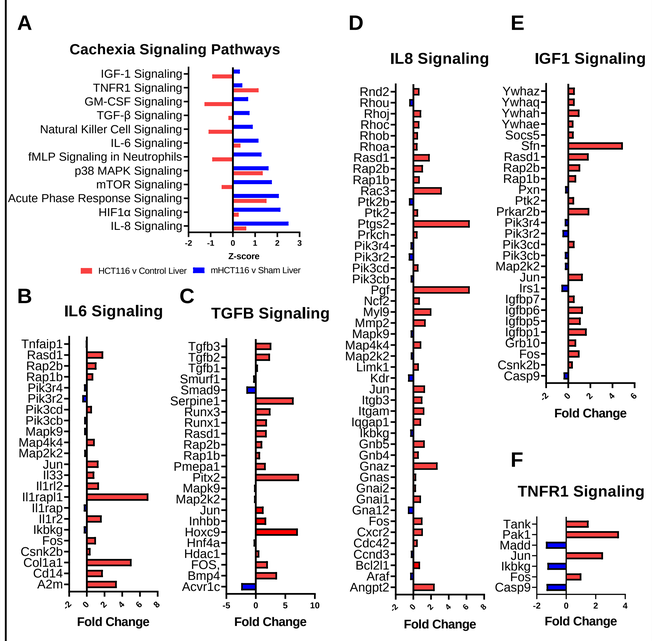

Figure 4: **(A)** Ingenuity Pathway Analysis was performed to determine activation Z-scores in canonical cancer cachexia associated signaling pathways for HCT116 vs. Control livers and mHCT116 vs. Sham livers comparisons. Fold change of factors annotating to selected cachexia signaling pathways including **(B)** IL6, **(C)** TGFB, **(D)** IL8, **(E)** IGF1, and **(F)** TNFR1 signaling pathways for mHCT116 vs. HCT116 livers. Control n=3, HCT116 n=3, Sham n=6, mHCT116 n=6

Figure 5: Adhesion and Gap junction molecules are upregulated with LMs in tumor and host

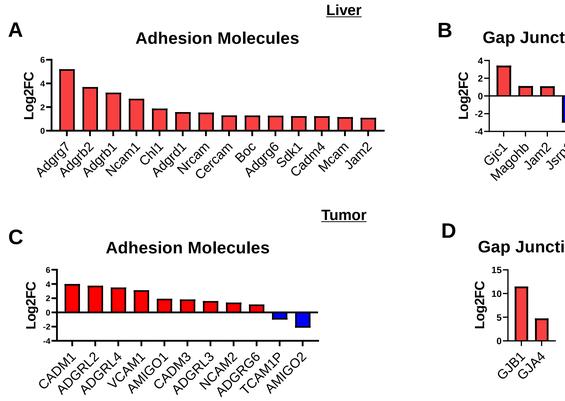

Figure 5: **(A)** Differentially expressed Adhesion and Gap Junction molecules in liver comparing mHCT116 vs HCT116 using a FDR-q threshold >.05. **(B)** Differentially expressed Adhesion and Gap Junction molecules in tumor comparing mHCT116 vs HCT116 using an FDR-q threshold >.05. HCT116 n=3, mHCT116 n=6

Figure 6: AML12 and HCT116 crosstalk is sufficient to activate cachexia signaling

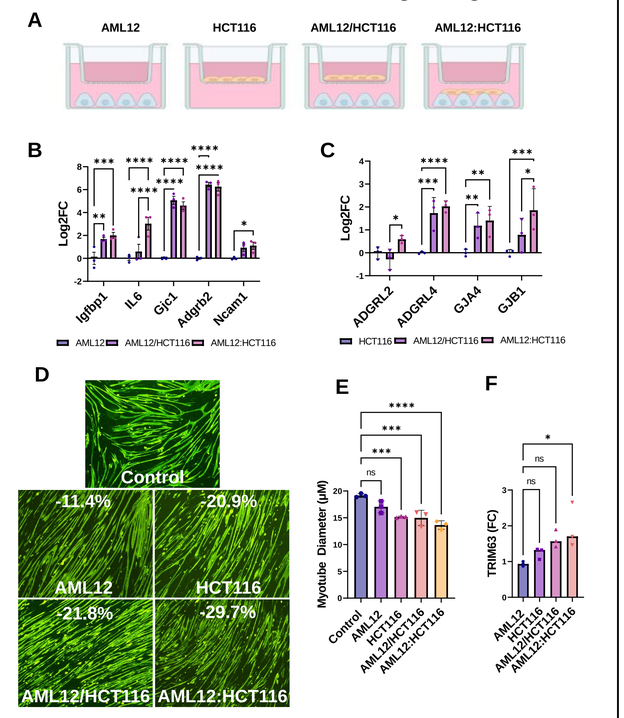

Figure 6: **(A)** AML12 hepatocytes co-cultured (by using permeable transwells) with HCT116 CRC cells for 48 hours (n=3). **(B)** AML12 gene expression profiling for cachexia (*Il6, Igfbp1*), gap junction (*Gjc1*), and Adhesion (*Adgrb2, Ncam1*) molecules. **(C)** HCT116 gene expression profiling for Adhesion (*ADGRL2, ADGRL4*) and Gap Junction (*GJA4, GJB1*) molecules. **(D)** C2C12 treated with conditioned media from AML12, HCT116, AML12/HCT116, or AML12:HCT116 for 48hrs and (E) myotube diameter was measured **(E)** *Trim63* mRNA expression in C2C12 following 2hr conditioned media treatment. Data are expressed as mean ± SD *p<0.05, **p<0.01, ***p<0.001, ****p<0.0001 vs. AML12 or HCT116

Conclusions

- LMs of CRC enhance activation of cachexia associated signaling pathways
- Worsened cachexia phenotype was coincident with upregulation in adhesion and gap junction molecules in liver and tumor
- Hepatocyte (AML12) and CRC (HCt116) co-culture recapitulates these effects in vitro
- ***→ Targeting LMs by disrupting cell-to-cell communication may present a viable strategy to reduce cachexia***

Acknowledgments

This study was supported by grants from the National Institute of Arthritis and Musculoskeletal and Skin Diseases (R01AR079379, R01AR080051), the Showalter Research Trust, The V Foundation for Cancer Research (V2017-021), the American Cancer Society (Research Scholar Grant 132013-RSG-18-010-01-CCG) to AB. JRH was supported by NIH/NIAMS through a T32 Institutional Training Grant (AR065971) and a Postdoctoral Fellowship (F32AR079256).